# *Limit equilibrium analysis and the minimum thickness of circular masonry arches to withstand lateral inertial loading*

**Haris Alexakis & Nicos Makris**

**Archive of Applied Mechanics**

ISSN 0939-1533
Volume 84
Number 5

Arch Appl Mech (2014) 84:757-772
DOI 10.1007/s00419-014-0831-4




Springer

Your article is protected by copyright and all rights are held exclusively by Springer-Verlag Berlin Heidelberg. This e-offprint is for personal use only and shall not be self-archived in electronic repositories. If you wish to self-archive your article, please use the accepted manuscript version for posting on your own website. You may further deposit the accepted manuscript version in any repository, provided it is only made publicly available 12 months after official publication or later and provided acknowledgement is given to the original source of publication and a link is inserted to the published article on Springer's website. The link must be accompanied by the following text: "The final publication is available at link.springer.com".



Author's personal copy

Arch Appl Mech (2014) 84:757–772
DOI 10.1007/s00419-014-0831-4

ORIGINAL

**Haris Alexakis · Nicos Makris**

# Limit equilibrium analysis and the minimum thickness of circular masonry arches to withstand lateral inertial loading

Received: 5 September 2013 / Accepted: 6 February 2014 / Published online: 28 February 2014
© Springer-Verlag Berlin Heidelberg 2014

**Abstract** In this paper, we compute the location of the imminent hinges and the minimum thickness, $t$, of a circular masonry arch with mid-thickness radius, $R$, and embracing angle, $\beta$, which can just sustain its own weight together with a given level of a horizontal ground acceleration, $\varepsilon\, g$. Motivated from the recent growing interest in identifying the limit equilibrium states of historic structures in earthquake prone areas, this paper shows that the value of the minimum horizontal acceleration that is needed to convert an arch with slenderness $(t/R, \beta)$ into a four-hinge mechanism depends on the direction of the rupture at the imminent hinge locations. This result is obtained with a variational formulation and the application of the principle of stationary potential energy, and it is shown that a circular arch becomes a mechanism with vertical ruptures when subjected to a horizontal ground acceleration that is slightly lower than the horizontal acceleration needed to create a mechanism with radial ruptures. The paper explains that the multiplicity on the solution for the minimum uplift acceleration is a direct consequence of the multiple possible ways that a masonry arch with finite thickness may rupture at a given location. The paper further confirms that the results obtained with commercially available distinct element software are in very good agreement with the rigorous solution.

**Keywords** Stone arches · Stereotomy · Minimum uplift acceleration · Limit state · Seismic analysis · Variational formulation · Earthquake engineering

## 1 Introduction

As early as in the first half of the eighteenth century, Couplet [1] presented a remarkably complete solution to the problem of computing the minimum thickness of a semicircular masonry arch with mid-thickness radius, $R$, and thickness, $t$, capable of supporting its own weight. His work brings forward in a most lucid way the two key concepts needed in the limit equilibrium analysis of masonry arches that do not sustain tension: (a) the limiting thrust line; and (b) the imminent mechanism of collapse. In his analysis, Couplet faces the challenge of computing the location of the intrados hinge of the five-hinge mechanism. He bypasses this problem by merely assuming that the rupture location is at $\varphi_r = 45^\circ = \pi/4$. In this way, Couplet forces the selection of the failure mechanism; therefore, his solution for the minimum thickness, $t/R = 0.101$, is unconservative, given that a neighboring mechanism might have developed at a larger thickness. The exact location of the

H. Alexakis · N. Makris (✉)
Department of Civil Engineering, University of Patras, 26500 Patras, Greece
E-mail: nmakris@upatras.gr

H. Alexakis
E-mail: alexakis@upatras.gr

N. Makris
Office of Theoretical and Applied Mechanics of the Academy of Athens, Athens, Greece

Author's personal copy



intrados hinge, $\varphi_r = 54.5°$, and the correct value of $t/R = 0.1075$ of the semicircular monolithic arch with zero tensile strength are computed rigorously for the first time by Milankovitch [2,3] some 175 years after Couplet's pioneering work.

While the analysis of masonry arches under static gravity loads has a long history and a rich literature ([4–7], and references reported therein), the analysis of masonry arches when subjected to lateral dynamic loads essentially starts with the seminal paper by Oppenheim [8].

The planar dynamic response of masonry arches that do not sustain tension can be analyzed in two steps. Step (a) is a static-equilibrium stability analysis and deals with the calculation of the minimum horizontal acceleration, $\ddot{u}_g^{\text{up}}$, that is needed to rupture an arch with an embrace angle $\beta$, mid-thickness radius $R$ and thickness $t$ at four locations (hinge formation) and induce rocking. Upon uplift has been induced, step (b) deals with the dynamic response analysis of the rocking arch by solving the nonlinear equations of motion, while addressing satisfactorily the impact which happens whenever the motion reverses.

Step (a) is a purely geometric problem which is independent of the scale (size $= R$) of the arch and depends solely on the slenderness of the arch $= (t/R,\ \beta)$. In analogy with the uplifting of a free-standing rectangular block (with base $= 2b$ and height $= 2h$) where the uplift horizontal acceleration is $\ddot{u}_g^{\text{up}}/g = b/h = \tan a$, the problem associated with step (a) for circular arches reduces to the derivation of the corresponding expression $\ddot{u}_g^{\text{up}}/g = f(t/R,\ \beta)$.

In the case of a free-standing rectangular column [9,10] or the case of a free-standing rocking frame [11], the derivation of the uplift acceleration $\ddot{u}_g^{\text{up}}/g = b/h$ is straightforward given that the location of the hinge formation is known a priory—that is the pivoting edges of the rectangular column. In the case of a circular arched monolith that is about to become a four-hinge mechanism and initiate rocking motion, the calculation of the uplift acceleration $\ddot{u}_g^{\text{up}}/g = f(t/R,\ \beta)$ is less straightforward since the location of the imminent hinges is unknown. Consequently, when studying the limit equilibrium of arches subjected to lateral loads, one faces the challenge to compute the location of the four hinges in a similar way as Couplet [1] faced the challenge to compute the location of the intrados hinge when the circular arch is subjected solely to its own gravity load.

Upon the locations of the hinges on the imminent mechanism of a circular arch $(R,\ t,\ \beta)$ have been established in step (a) together with the rupture/uplift acceleration $\ddot{u}_g^{\text{up}}/g = f(t/R,\ \beta)$, the arch may rock as a one-degree-of-freedom, four-link mechanism. The nonlinear dynamic response of the arch examined in the second step (b) depends not only on the slenderness of the arch $(t/R,\ \beta)$ but also on the size of the arch, $R$, as has been shown by Oppenheim [8], Clemente [12] and further confirmed by De Lorenzis et al. [13] and DeJong et al. [14].

In this paper, we revisit step (a) and compute rigorously the value of the rupture/uplift acceleration of circular arches with slenderness $(t/R,\ \beta)$ after identifying the exact locations of the four imminent hinges by adopting a variational formulation via the application of the principle of stationary potential energy. The paper shows that the value of the minimum horizontal acceleration that is needed to convert an arch with slenderness $(t/R,\ \beta)$ into a four-hinge mechanism depends on the direction of the rupture at the hinge locations—that is the answer depends on the stereotomy exercised on the arch.

In his pioneering study, Oppenheim [8] did not consider a continuous monolithic arch with zero tensile strength, but rather a circular arch that consists of seven (7) voussoirs having eight (8) radial joints. Accordingly, the imminent hinges in Oppenheim's arch can only occur at the predefined locations of the eight physical joints; therefore, Oppenheim's arch allows for the development of a finite number of physically admissible mechanisms, while excludes neighboring mechanisms that might have developed in the continuous monolithic arch at a lower lateral load. For instance, Oppenheim [8] reports that "…in an arch with $t/R = 0.10$, the governing mechanism has hinges at positions $-5, -1, 3, 7$ at which the minimum horizontal ground acceleration for onset of motion equals $0.196\ g$." Clearly, this result is relevant only to the 7-voussoir arch with radial joints and angle of embrace $\beta = 157.5°$.

While Oppenheim [8] recognizes that the critical mechanism of a masonry arch with a given sufficient thickness $t/R$ is the one which is mobilized by the lowest horizontal ground acceleration, no explanation is offered on how he selects the "theoretical governing mechanism" with hinges at positions $-7$, $-1$, 3 and 7. Figure 1 plots the minimum uplift acceleration for semicircular arches as computed by Oppenheim [8] for the 7-voussoir arch together with the exact solution for the continuous circular monolith computed in this paper with a variational formulation after adopting that the rupture at the location of the imminent hinges occurs along the radial direction. The results reported by Oppenheim [8] are slightly above the minimum uplift acceleration values of the continuous monolith given that in Oppenheim's 7-voussoir arch, hinges are allowed to form only at the distinct locations of the 8 physical joints. Together with the uplift acceleration values of the semicircular arch with slenderness $(t/R,\ \beta)$, Fig. 1 also plots the uplift acceleration of the rectangular

Author's personal copy



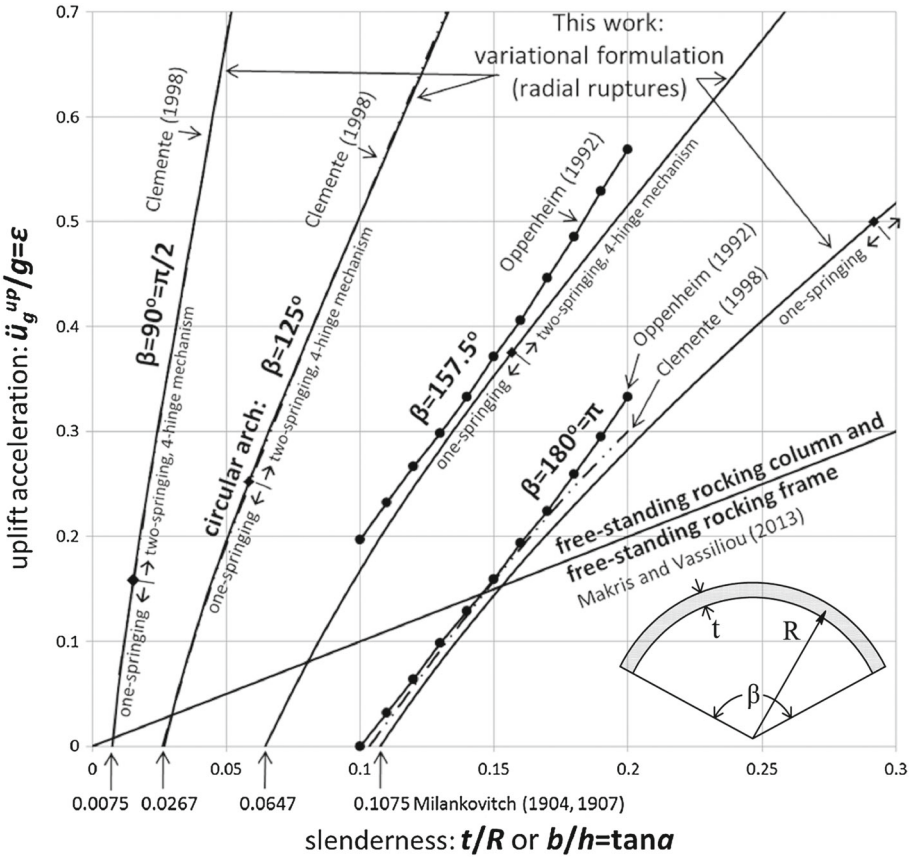



**Fig. 1** Minimum uplift horizontal acceleration of a circular arch with angle of embrace $\beta$ and slenderness $t/R$. The rigorous solution derived in this work with a variational formulation (*solid lines*) after adopting radial ruptures at the location of the imminent hinges is compared with the results obtained by Oppenheim [8] for a 7-voussoir arch and by Clemente [12]

free-standing block with slenderness $b/h = \tan a$. Figure 1 shows that once the circular arch is thick enough to support its own weight ($t/R > 0.0075$ for $\beta = 90°$, $t/R > 0.0267$ for $\beta = 125°$, $t/R > 0.0647$ for $\beta = 157.5°$, $t/R > 0.1075$ for $\beta = \pi$), the horizontal acceleration $\ddot{u}_g^{up}$ that is needed to induce rocking motion increases much more rapidly with slenderness than the horizontal acceleration that is needed to induce rocking to the free-standing rocking frame [11]. This comparison contributes to the understanding of the seismic stability of the buttress arch as formulated by De Luca et al. [15].

Clemente [12] further elaborated on the dynamic response and stability analysis of masonry arches subjected to a horizontal ground acceleration. In Clemente's work, the hinge mechanism and the value of the ground acceleration needed to initiate rocking are found by employing an iterative procedure which assumes an initial mechanism which is iteratively adjusted by satisfying simultaneously the principle of virtual powers and that in the converged mechanism the corresponding thrust line can just be located within the profile of the arch. Consequently, Clemente's [12] iterative method mixes elements from energy methods and from a geometric formulation which involves the limiting thrust line. Figure 1 plots with a chain line the minimum uplift acceleration for a continuous monolithic circular arch with slenderness $t/R$ and $\beta = 90°$, 125° and 180° as computed by Clemente [12] next to the results computed by Oppenheim [8] for the 7-voussoir arch with $\beta = 157.5°$ and $\beta = 180°$. Clemente's [12] results are in excellent agreement with the rigorous solution derived in this paper with a variational formulation after assuming ruptures along the radial direction.

What is remarkable in Clemente's work is that he recognizes that when a masonry arch is subjected to a lateral load (say to the right), the extreme right hinge will happen at the right springing A, while the extreme left hinge D may happen within the arch at a location above the left springing. Accordingly, depending on the slenderness of the arch ($t/R$, $\beta$) and the level of the horizontal ground acceleration, the circular arch may develop a one- springing or a two-springing, 4-hinge mechanism as shown in Fig. 2.

Author's personal copy



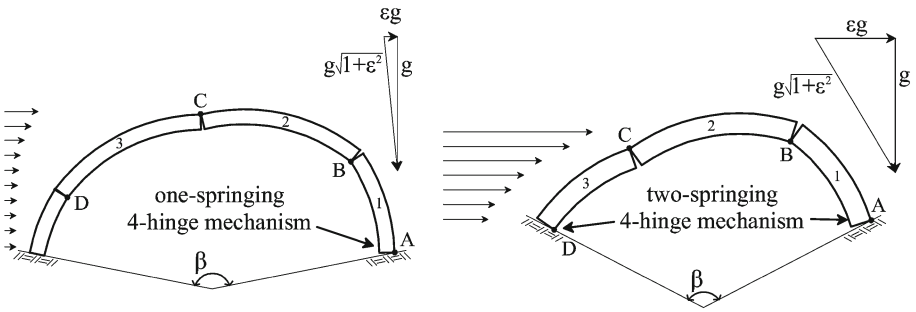



**Fig. 2** Depending on the value of the embracing angle $\beta$, the thickness of the arch $t/R$ and the intensity of the horizontal acceleration $\varepsilon\, g$, the four-hinge mechanism will hinge either only at one (*left*) or at both springings (*right*)

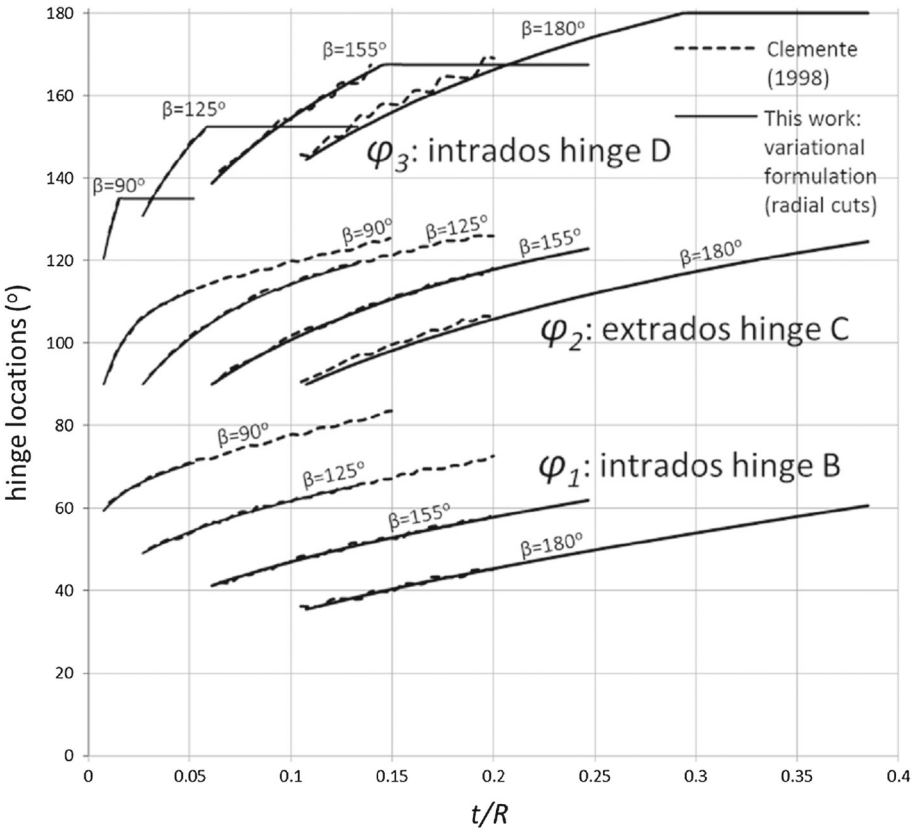



**Fig. 3** Location of the imminent hinges $\varphi_1$, $\varphi_2$, and $\varphi_3$ at points B, C and D, respectively, of a circular arch with a given angle of embrace $\beta$ and slenderness $t/R$. The rigorous solution derived in this work with a variational formulation (*solid lines*) after adopting radial ruptures at the locations of the imminent hinges is compared with the results obtained by Clemente [12]

Figure 3 plots with a dashed line the locations of the imminent hinges $\varphi_1$, $\varphi_2$ and $\varphi_3$ at points B, C and D, respectively (see also Fig. 4) of a continuous monolithic arch with slenderness $t/R$ and $\beta = 90°$, 125°, 155° and 180°, as computed by Clemente [12]. In his paper, Clemente focuses on presenting the hinge locations of a one-springing, 4-hinge mechanism, and therefore, Clemente's graph for the third hinge $\varphi_3$ does not include the flat portion shown in Fig. 3 which corresponds to the case where a two-springing, 4-hinge mechanism develops ($\varphi_3 = \beta + (\pi\text{-}\beta)/2 = (\beta + \pi)/2$). Figure 3 confirms that Clemente's [12] results are in excellent agreement with the rigorous solution derived in this paper with a variational formulation after assuming ruptures along the radial direction.

Ochsendorf [16] built upon Clemente's [12] work and developed an alternative iterative process to identify the collapse mechanism and the minimum acceleration needed to rupture/uplift a circular arch. Knowing that the downstream extreme hinge of the 4-hinge mechanism is at the springing of the arch, Ochsendorf [16]

Author's personal copy



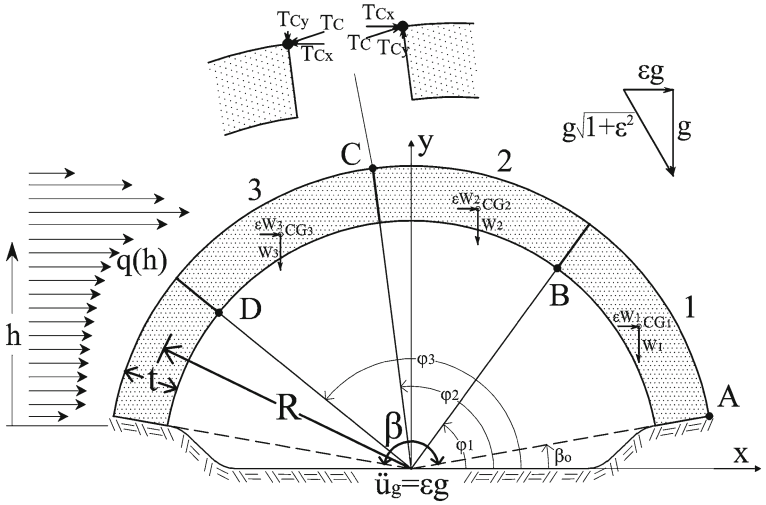



**Fig. 4** Formation of a four-hinge mechanism in a circular arch $(R,\ t,\ \beta)$ when subjected to a horizontal ground acceleration $\ddot{u}_g = \varepsilon g$. The direction of the ruptures at the hinge locations is assumed radial

initially assumes the locations of the other three hinges and subsequently computes the level of the horizontal acceleration that satisfies the principle of virtual work. This calculation is repeated at a neighboring location of the assumed hinges until the process converges to the lowest value of the horizontal acceleration which can mobilize a kinematically admissible mechanism. Ochsendorf [16] iterative process is essentially a numerical exercise that emulates in a step-by-step fashion the fundamental concept of variational calculus (each new numerical iteration in Ochsendorf's software involves a finite variation of the hinge locations) from which derives the principle of stationary potential energy.

In this paper, we present a straightforward application of the principle of stationary potential energy to compute the value of the rupture/uplift acceleration of circular arches together with the exact locations of the four imminent hinges. This rigorous variational formulation shows that the exact value of the rupture/uplift acceleration depends on the stereotomy exercised [17–19] and settles the problem of the limit equilibrium analysis of masonry arches within the formal theory of energy methods without the need to involve the geometric concept of the thrust line.

## 2 Identification of the imminent four-hinge mechanism and the minimum thickness needed to sustain a given horizontal acceleration

Consider the circular arch $(R,\ t,\ \beta)$ with mid-thickness radius $R$, thickness $t$, and angle of embrace $\beta$, subjected to a constant horizontal ground acceleration $\varepsilon\, g$. Prior to hinging, the arch translates as a rigid body, and therefore, the lateral inertial loading will assume a profile proportional to the vertical distribution of the mass of the circular arch as shown in Fig. 4. For thin arches, this distribution can be approximated with $q(h) = \varphi/\sin\varphi$. When the horizontal inertial loading is sufficiently large, the arch will become a four-hinge mechanism. With reference to Fig. 4, Clemente [12] has shown that the downstream hinge, A, forms at the extrados of the springing which is at $\beta_o = (\pi - \beta)/2$ and the associated kinematic admissible mechanism has an intrados hinge B at the unknown location $\varphi_1$, an extrados hinge C at the unknown location $\varphi_2$ and an intrados upstream hinge D at the unknown location $\varphi_3$. In this work, the location of the hinges is identified with the application of the principle of stationary potential energy, and therefore, the weights of the articulated portions of the arch need to be computed.

### 2.1 Radial ruptures: variational formulation

At this stage, we face the selection of the direction of the imminent ruptures that will initiate at points B, C and D. Perhaps the most natural assumption is a radial rupture given that it has the shortest length among all possible rupture directions.

Author's personal copy



With the adoption of radial ruptures, the weights $W_2$ and $W_3$ of segment 2 (segment BC) and segment 3 (segment CD) of the arch are given by

$$W_2 = tR\,(\phi_2 - \phi_1) \tag{1}$$
$$W_3 = tR\,(\phi_3 - \phi_2) \tag{2}$$

while the weight of the combined segments 1–2 (segment ABC) is given by

$$W_{1-2} = tR(\phi_2 - \beta_o) \tag{3}$$

Furthermore, the coordinates of the centers of gravity of these segments are given by

$$x_{o2} = R\frac{\sin\phi_2 - \sin\phi_1}{\phi_2 - \phi_1}\left(1 + \frac{1}{12}\frac{t^2}{R^2}\right), \quad y_{o2} = -R\frac{\cos\phi_2 - \cos\phi_1}{\phi_2 - \phi_1}\left(1 + \frac{1}{12}\frac{t^2}{R^2}\right) \tag{4}$$
$$x_{o3} = R\frac{\sin\phi_3 - \sin\phi_2}{\phi_3 - \phi_2}\left(1 + \frac{1}{12}\frac{t^2}{R^2}\right), \quad y_{o3} = -R\frac{\cos\phi_3 - \cos\phi_2}{\phi_3 - \phi_2}\left(1 + \frac{1}{12}\frac{t^2}{R^2}\right) \tag{5}$$
$$x_{o1-2} = R\frac{\sin\phi_2 - \sin\beta_o}{\phi_2 - \beta_o}\left(1 + \frac{1}{12}\frac{t^2}{R^2}\right), \quad y_{o1-2} = -R\frac{\cos\phi_2 - \cos\beta_o}{\phi_2 - \beta_o}\left(1 + \frac{1}{12}\frac{t^2}{R^2}\right) \tag{6}$$

Moment equilibrium of the combined segment 1–2 (segment ABC) about hinge A gives

$$\begin{aligned}&\varepsilon W_{1-2}\left[y_{o1-2} - \sin\beta_o\left(R + \frac{t}{2}\right)\right] - W_{1-2}\left[\cos\beta_o\left(R + \frac{t}{2}\right) - x_{o1-2}\right]\\ &+ T_{Cx}(\sin\phi_2 - \sin\beta_o)\left(R + \frac{t}{2}\right) + T_{Cy}(\cos\beta_o - \cos\phi_2)\left(R + \frac{t}{2}\right) = 0\end{aligned} \tag{7}$$

In Eq. (7), the forces $T_{Cx}$ and $T_{Cy}$ are the cartesian components of the internal trust force $T_C$ acting at the hinge C. It is worth mentioning that the thrust line of the arch that is about to become a mechanism is tangent to the extrados of the arch at point C; when one works with a polar coordinate system and assumes radial ruptures, the thrust force $T_C$ is not tangent to the thrust line (therefore not tangent to the extrados of the arch). This subtle piece of knowledge was apparently known since the seminal paper of Lamé and Clapeyron [20] (see also [17,18,21,22]) and was proven rigorously by Milankovitch [2,3] who made a clear distinction between the "druckkurve" and the "stützlinie" (see also [6]). Consequently, given that $T_C$ is not tangent to the extrados, both its magnitude and direction are unknowns (or both $T_{Cx}$ and $T_{Cy}$ are unknowns).

Moment equilibrium of segment 2 (segment BC) about hinge B gives

$$\begin{aligned}&\varepsilon W_2\left[y_{o2} - \sin\phi_1\left(R - \frac{t}{2}\right)\right] - W_2\left[\cos\phi_1\left(R - \frac{t}{2}\right) - x_{o2}\right]\\ &+T_{Cx}\left[\sin\phi_2\left(R + \frac{t}{2}\right) - \sin\phi_1\left(R - \frac{t}{2}\right)\right] + T_{Cy}\left[\cos\phi_1\left(R - \frac{t}{2}\right) - \cos\phi_2\left(R + \frac{t}{2}\right)\right] = 0\end{aligned} \tag{8}$$

while moment equilibrium of segment 3 (segment CD) about hinge D gives

$$\begin{aligned}&\varepsilon W_3\left[y_{o3} - \sin\phi_3\left(R - \frac{t}{2}\right)\right] + W_3\left[x_{o3} - \cos\phi_3\left(R - \frac{t}{2}\right)\right]\\ &-T_{Cx}\left[\sin\phi_2\left(R + \frac{t}{2}\right) - \sin\phi_3\left(R - \frac{t}{2}\right)\right] + T_{Cy}\left[\cos\phi_2\left(R + \frac{t}{2}\right) - \cos\phi_3\left(R - \frac{t}{2}\right)\right] = 0\end{aligned} \tag{9}$$

Substitution of Eqs. (8) and (9) into (7) eliminates the unknown components $T_{Cx}$ and $T_{Cy}$ and yields a transcendental equation which involves the five quantities $t/R$, $\varphi_1$, $\varphi_2$, $\varphi_3$ and $\varepsilon$. In the event of a capacity design (find the size of the structure that can sustain a given loading), the seismic coefficient $\varepsilon$ is given and the minimum thickness of the arch $t/R$ is unknown. In the event of a demand assessment (find the level of loading that a given structure can sustain), the thickness of the arch $t/R$ is given and the seismic coefficient $\varepsilon$ is unknown. As an example, Fig. 1 is organized in the context of a demand assessment. Consider the case of a capacity

Author's personal copy



design (find $t/R$); therefore, the solution of the above mentioned transcendental equation can be expressed in the form

$$t/R = f(\phi_1, \phi_2, \phi_3, \varepsilon) \tag{10}$$

where $\varepsilon$ is now the given seismic coefficient ($\ddot{u}_g = \varepsilon\, g$), and $\varphi_1$, $\varphi_2$ and $\varphi_3$ are the unknown hinge locations of the imminent 4-hinge mechanism (the fourth hinge has a known location at the "downstream" springing A that is at $\beta_o$).

Our analysis proceeds with the application of the principle of stationary potential energy by adopting as a reference level the horizontal axis $x$ ($y = 0$) as shown in Fig. 5. With reference to this level ($y = 0$), the potential energy of the circular arch ($R$, $t$, $\beta$) is

$$V = W y_o = 2 \sin\left(\frac{\beta}{2}\right) R^3 \frac{t}{R}\left(1 + \frac{1}{12}\frac{t^2}{R^2}\right) \tag{11}$$

Substitution of Eq. (10) into Eq. (11), the potential energy of the circular arch is expressed as

$$V(\phi_1, \phi_2, \phi_3, \varepsilon) = 2 \sin\left(\frac{\beta}{2}\right) R^3 f(\phi_1, \phi_2, \phi_3, \varepsilon)\left[1 + \frac{1}{12} f(\phi_1, \phi_2, \phi_3, \varepsilon)^2\right] \tag{12}$$

The structural system shown in Fig. 5 (left) is a case where the forces (vertical weight and horizontal inertial forces) acting on the system are conservative. Furthermore, given the equivalent static representation of the horizontal acceleration $\varepsilon\, g$ adopted in this paper, the resultant acceleration field $g\sqrt{1+\varepsilon^2}$ is inclined at an angle $\omega$ from the vertical such that $\tan\omega = \varepsilon$. Consequently, the loading on a circular masonry arch subjected to a horizontal acceleration $\varepsilon\, g$ is equivalent to the gravity loading on the same arch when tilted at an angle $\omega = \tan^{-1}\varepsilon$ from the vertical, subjected to a gravitational field $\widehat{g} = g\sqrt{1+\varepsilon^2}$ [16,23,24]. Concentrating on the tilting arch shown in Fig. 5 (right), the ordinate of its center of gravity relative to the level $y = 0$ is $\widehat{y} = y_o \cos\omega = y_o/\sqrt{1+\varepsilon^2}$, while its weight is $\widehat{W} = W\sqrt{1+\varepsilon^2}$ given the enhancement of the gravitational field. Consequently, in the tilted configuration shown in Fig. 5 (right), the potential energy of the arch relative to the level $y = 0$ is

$$\widehat{V} = \widehat{W} \cdot \widehat{y} = W\sqrt{1+\varepsilon^2}\,\frac{y_o}{\sqrt{1+\varepsilon^2}} = W \cdot y_o = V \tag{13}$$

Equation (13) shows that the potential energy of the tilting arch is equal to potential energy of the leveled arch in its original configuration. Consequently, for the tilting arch shown in Fig. 5 (right), the work of all forces is accounted by the potential energy $V(\varphi_1, \varphi_2, \varphi_3, \varepsilon)$ given by Eq. (12). According to the principle of stationary potential energy, the geometrically admissible hinged mechanism shown in Fig. 4 is in an equilibrium state if and only if the total potential energy of the arch is stationary ($\delta V = 0$). Since in this case, the potential energy $V(\varphi_1, \varphi_2, \varphi_3, \varepsilon)$ is a function of three variables $\varphi_1$, $\varphi_2$ and $\varphi_3$, the potential energy is stationary when [25, among others]

$$\frac{\partial V(\phi_1, \phi_2, \phi_3, \varepsilon)}{\partial \phi_1} = 0 \tag{14}$$

$$\frac{\partial V(\phi_1, \phi_2, \phi_3, \varepsilon)}{\partial \phi_2} = 0 \tag{15}$$

and

$$\frac{\partial V(\phi_1, \phi_2, \phi_3, \varepsilon)}{\partial \phi_3} = 0 \tag{16}$$

Substitution of Eq. (12) to any of the Eqs. (14)–(16) ($j \in \{1, 2, 3\}$) gives

$$\frac{\partial V(\phi_j, \varepsilon)}{\partial \phi_j} = 2 \sin\left(\frac{\beta}{2}\right) R^3 \frac{\partial f(\phi_j, \varepsilon)}{\partial \phi_j}\left[1 + \frac{1}{4} f(\phi_j, \varepsilon)^2\right] = 0, \quad j \in \{1, 2, 3\} \tag{17}$$

Author's personal copy



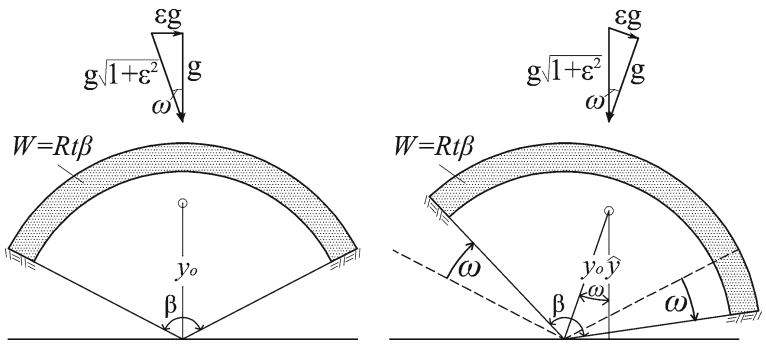



**Fig. 5** The stress state of the leveled arch (*left*) subjected to its gravity load, and a constant horizontal acceleration $\varepsilon g$ is identical to the stress state of the tilted arch by an angle $\omega = \tan^{-1}\varepsilon$ (*right*) subjected to a gravitational field with intensity $g\sqrt{1+\varepsilon^2}$

The quantity in brackets in Eq. (17) is always positive; therefore, Eq. (17) is satisfied only when $\frac{\partial f(\phi_j,\varepsilon)}{\partial \phi_j} = 0$. Accordingly, the tilting arch is in limiting equilibrium state ($\delta V(\varphi_1, \varphi_2, \varphi_3, \varepsilon) = 0$) if and only if all partial derivatives of the function $f(\varphi_1, \varphi_2, \varphi_3, \varepsilon)$ given by Eq. (10) vanish

$$\frac{\partial f(\phi_1, \phi_2, \phi_3, \varepsilon)}{\partial \phi_1} = \frac{\partial (t/R)}{\partial \phi_1} = 0 \tag{18}$$

$$\frac{\partial f(\phi_1, \phi_2, \phi_3, \varepsilon)}{\partial \phi_2} = \frac{\partial (t/R)}{\partial \phi_2} = 0 \tag{19}$$

$$\frac{\partial f(\phi_1, \phi_2, \phi_3, \varepsilon)}{\partial \phi_3} = \frac{\partial (t/R)}{\partial \phi_3} = 0 \tag{20}$$

Numerical solution of the system of Eqs. (10) and (18)–(20) gives the unknown locations $\varphi_1$, $\varphi_2$ and $\varphi_3$ of the three hinges (the location of the fourth hinge is known at the downstream springing A) together with the minimum thickness $t/R$ of a circular arch with a given angle of embrace $\beta$.

Figure 6 plots with a solid line the minimum thickness values $t/R$ of a circular arch with a given angle of embrace $\beta$ when subjected to various levels of horizontal acceleration $\ddot{u}_g = \varepsilon\, g$. Note that the minimum thickness needed reduces appreciably as the embrace angle reduces. For instance, when $\beta = 125°$, a circular arch with $t/R = 0.1$ can withstand its own weight together with a horizontal acceleration of $\ddot{u}_g = 0.5g$ ($\varepsilon = 0.5$).

Figure 7 plots the location of the imminent hinges of a circular arch with a given angle of embrace $\beta$ when subjected to various levels of horizontal acceleration $\ddot{u}_g = \varepsilon g$ and when the direction of the ruptures is assumed radial.

## 2.2 Vertical ruptures: variational formulation

When the arch reaches its limit state and the formation of the four-hinge mechanism is imminent, the application of the principle of stationary potential energy requires the calculation of the weight of the articulated portions of the arch. In the previous section, we assumed that the ruptures that initiate at points B, C and D shown in Fig. 4 will develop along the radial direction. In this section, we assume that the ruptures that initiate at points B, C and D shown in Fig. 8 will develop along the vertical direction at the unknown locations $x_1$, $x_2$ and $x_3$.

With the adoption of vertical ruptures, the weights $W_2$ and $W_3$ of segment 2 (segment BC) and segment 3 (segment DC) of the arch are given by

$$W_2 = \int_{X_2}^{X_1} y_{\text{ex}}(x)\mathrm{d}x - \int_{X_2}^{X_1} y_{\text{in}}(x)\mathrm{d}x \tag{21}$$

$$W_3 = \int_{X_3}^{X_2} y_{\text{ex}}(x)\mathrm{d}x - \int_{X_3}^{X_2} y_{\text{in}}(x)\mathrm{d}x \tag{22}$$

Author's personal copy



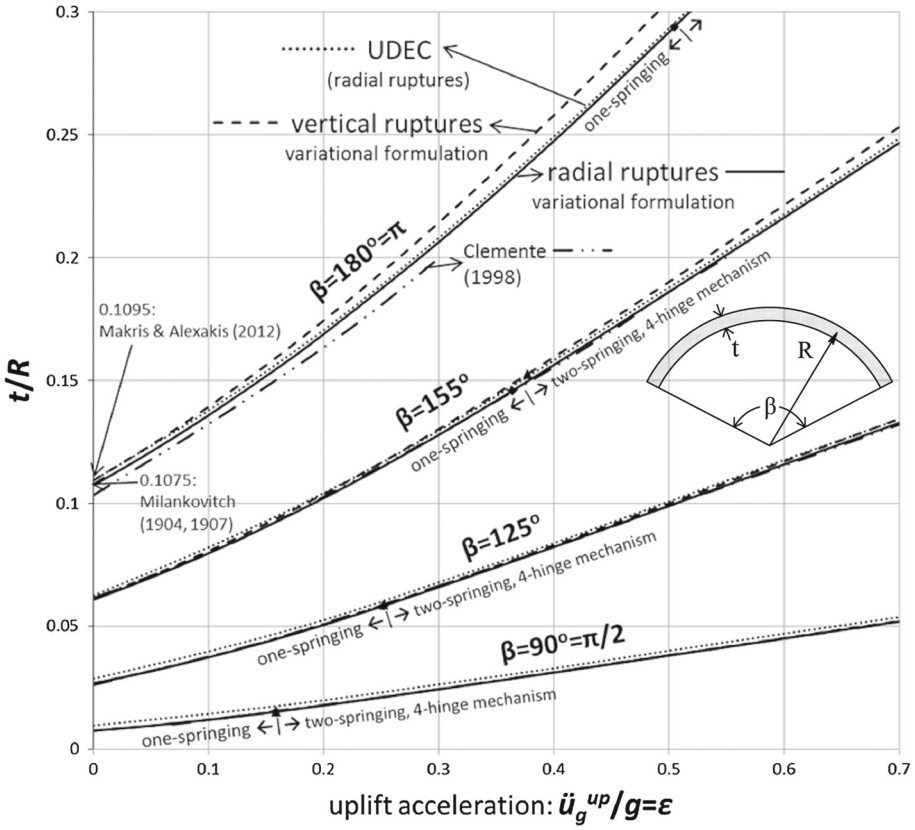



**Fig. 6** Minimum thickness values, *t/R*, of a circular arch with embrace angle, $\beta$, needed to withstand a constant horizontal acceleration $\ddot{u}_g = \varepsilon g$. The rigorous solution derived in this work with a variational formulation for either radial or vertical ruptures is compared with the results obtained by Clemente [12] (*chain line*) and the results obtained with the commercially available software UDEC [26]. For smaller embracing angles, $\beta$, the minimum thickness of the arches decreases and the differences between the solutions obtained with radial or vertical ruptures decreases

where $y_{\text{in}}(x)$ and $y_{\text{ex}}(x)$ are the ordinate of intrados and extrados of the arch expressed in cartesian coordinates

$$y_{\text{in}}(x) = \sqrt{\left(R - \frac{t}{2}\right)^2 - x^2} \tag{23}$$

$$y_{\text{ex}}(x) = \sqrt{\left(R + \frac{t}{2}\right)^2 - x^2} \tag{24}$$

The weight of the combined segment 1–2 (segment ABC) is given by

$$W_{1-2} = \left( \int_{X_2}^{X\text{Ain}} y_{\text{ex}}(x)\mathrm{d}x - \int_{X_2}^{X\text{Ain}} y_{\text{in}}(x)\mathrm{d}x \right) + \left( \int_{X\text{Ain}}^{X\text{A}} y_{\text{ex}}(x)\mathrm{d}x - \int_{X\text{Ain}}^{X\text{A}} \cot\left(\frac{\beta}{2}\right) x\mathrm{d}x \right) \tag{25}$$

where $x_{\text{A}}$ is the known abscissa of the "downstream" springing hinge at the extrados and $x_{\text{Ain}}$ is the abscissa of the springing point at the intrados

$$x_{\text{Ain}} = \sin\left(\frac{\beta}{2}\right)\left(R - \frac{t}{2}\right), \quad x_{\text{A}} = \sin\left(\frac{\beta}{2}\right)\left(R + \frac{t}{2}\right) \tag{26}$$

Author's personal copy



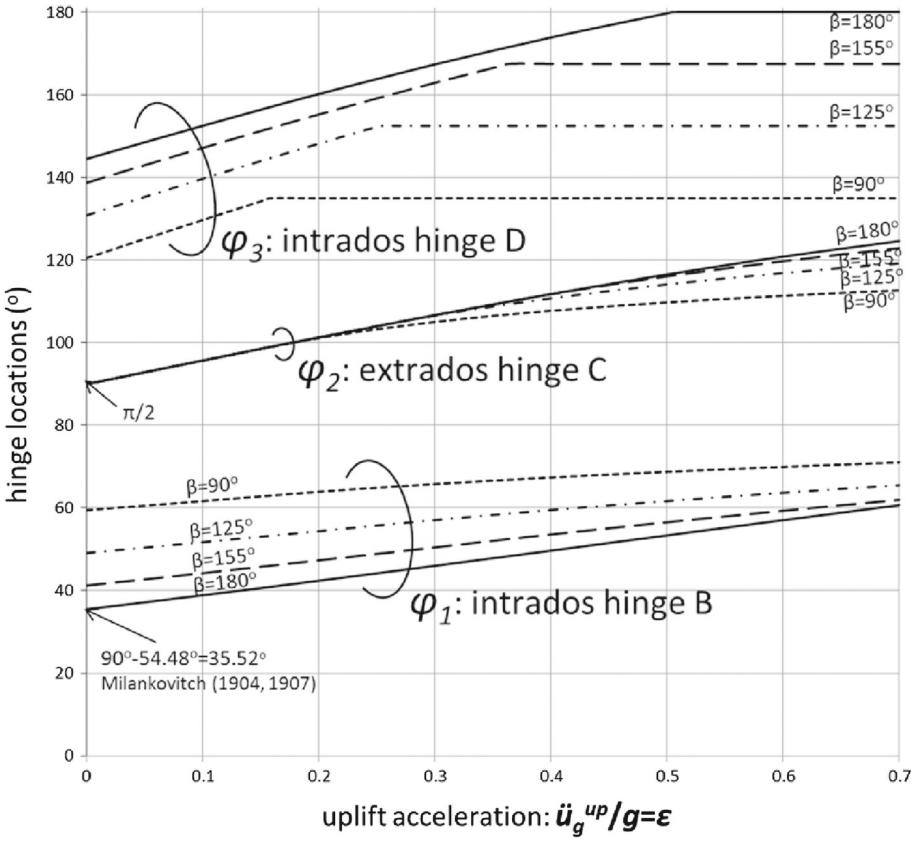



**Fig. 7** Location of the imminent hinges $\varphi_1$, $\varphi_2$, and $\varphi_3$, at points B, C and D of a circular arch with embrace angle $\beta$ and minimum thickness $t/R$ as shown in Fig. 6 (*solid lines*) that ruptures along the radial direction when subjected to a constant horizontal acceleration $\ddot{u}_g = \varepsilon g$

Furthermore, the coordinates of the centers of gravity of these articulated segments are given by

$$x_{o2} = \frac{\int_{X_2}^{X_1} y_{ex}(x)x\,dx - \int_{X_2}^{X_1} y_{in}(x)x\,dx}{W_2}, \quad y_{o2} = \frac{\int_{X_2}^{X_1} \frac{y_{ex}(x)^2}{2}dx - \int_{X_2}^{X_1} \frac{y_{in}(x)^2}{2}dx}{W_2} \tag{27}$$

$$x_{o3} = \frac{\int_{X_3}^{X_2} y_{ex}(x)x\,dx - \int_{X_3}^{X_2} y_{in}(x)x\,dx}{W_3}, \quad y_{o3} = \frac{\int_{X_3}^{X_2} \frac{y_{ex}(x)^2}{2}dx - \int_{X_3}^{X_2} \frac{y_{in}(x)^2}{2}dx}{W_3} \tag{28}$$

$$\begin{aligned} x_{o1-2} &= \frac{\left(\int_{X_2}^{X_{Ain}} y_{ex}(x)x\,dx - \int_{X_2}^{X_{Ain}} y_{in}(x)x\,dx\right) + \left(\int_{X_{Ain}}^{X_A} y_{ex}(x)x\,dx - \int_{X_{Ain}}^{X_A} \cot\left(\frac{\beta}{2}\right)x^2 dx\right)}{W_{1-2}} \\ y_{o1-2} &= \frac{\left(\int_{X_2}^{X_{Ain}} \frac{y_{ex}(x)^2}{2}dx - \int_{X_2}^{X_{Ain}} \frac{y_{in}(x)^2}{2}dx\right) + \left(\int_{X_{Ain}}^{X_A} \frac{y_{ex}(x)^2}{2}dx - \int_{X_{Ain}}^{X_A} \frac{\left(\cot\left(\frac{\beta}{2}\right)x\right)^2}{2}dx\right)}{W_{1-2}} \end{aligned} \tag{29}$$

Moment equilibrium of the combined segment 1–2 (segment ABC) about hinge A gives

$$\varepsilon W_{1-2}[y_{o1-2} - y_{ex}(x_A)] - W_{1-2}(x_A - x_{o1-2}) + T_{Cx}[y_{ex}(x_2) - y_{ex}(x_A)] + T_{Cy}(x_A - x_2) = 0 \tag{30}$$

In Eq. (30), the forces $T_{Cx}$ and $T_{Cy}$ are the cartesian components of the internal thrust force $T_C$ acting at the hinge C. It is worth mentioning that in the limit equilibrium analysis of arches under gravity (vertical) loads

Author's personal copy



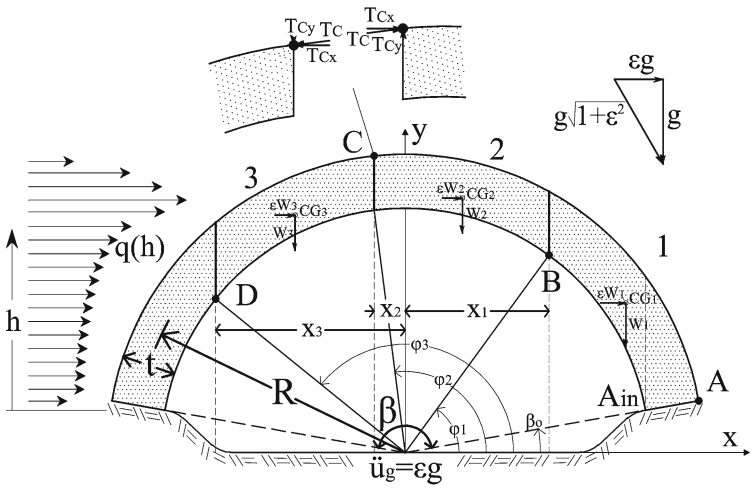



**Fig. 8** Formation of a four-hinge mechanism in a circular arch ($R$, $t$, $\beta$) when subjected to a horizontal ground acceleration $\ddot{u}_g = \varepsilon g$. The direction of the ruptures at the hinge locations is assumed vertical

alone, when one works with vertical cuts, the thrust force, $T_C$, is tangent to the thrust line [2,3]. This subtle piece of knowledge was apparently known since the work of Lamé and Clapeyron [20] (see also [17,18,21,22]). Nevertheless, in this case given the pressure of the horizontal inertial load ($\varepsilon\, g$), the vertical ruptures shown in Fig. 8 are not parallel to the resultant field force $g\sqrt{1+\varepsilon^2}$. Consequently, given the inclined field force $g\sqrt{1+\varepsilon^2}$, even for this case where we assume vertical ruptures, the thrust force $T_C$ is not tangent to the extrados; therefore, both its magnitude and direction are unknowns (or both $T_{Cx}$ and $T_{Cy}$ are unknowns). Accordingly, moment equilibrium of segment 2 (segment BC) about hinge B gives

$$\varepsilon W_2[y_{o2} - y_{in}(x_1)] - W_2(x_1 - x_{o2}) + T_{Cx}[y_{ex}(x_2) - y_{in}(x_1)] + T_{Cy}(x_1 - x_2)] = 0 \tag{31}$$

while moment equilibrium of segment 3 (segment CD) about hinge C gives

$$\varepsilon W_3[y_{o3} - y_{in}(x_3)] + W_3(x_{o3} - x_3) - T_{Cx}[y_{ex}(x_2) - y_{in}(x_3)] + T_{Cy}(x_2 - x_3) = 0 \tag{32}$$

Substitution of Eqs. (31) and (32) into (30) eliminates the unknown components $T_{Cx}$ and $T_{Cy}$ and yields a transcendental equation which involves the five quantities $t/R$, $x_1$, $x_2$, $x_3$ and $\varepsilon$. As explained earlier, in the event of a capacity design (find the size of the structure that can sustain a given loading) the seismic coefficient, $\varepsilon$, is given and the minimum thickness of the arch, $t/R$, is unknown. In the event of a demand assessment (find the level of loading that a given structure can sustain), the thickness of the arch, $t/R$, is given and the seismic coefficient $\varepsilon$ is unknown.

Let us consider now the case of a capacity design (find $t/R$); therefore, the solution of the abovementioned transcendental equation is expressed in the form

$$t/R = f(x_1, x_2, x_3, \varepsilon) \tag{33}$$

where $\varepsilon$ is now the given seismic coefficient ($\ddot{u}_g = \varepsilon\, g$) and $x_1$, $x_2$ and $x_3$ are the unknown hinge locations of the four-hinge mechanism (the forth hinge has a known location at the "downstream" springing A that is at $x_A = \sin\left(\frac{\beta}{2}\right)\left(R + \frac{t}{2}\right)$.

Our analysis proceeds again with the application of the principle of stationary potential energy by adopting as a reference level the horizontal axis $x$ ($y = 0$) as shown in Fig. 8. With reference to this level ($y = 0$), the potential energy of the circular arch ($R$, $t$, $\beta$) is given by Eq. (11). Substitution of Eq. (33) into Eq. (11), the potential energy of the leveled circular arch is now expressed as

$$V(x_1, x_2, x_3, \varepsilon) = 2\sin\left(\frac{\beta}{2}\right) R^3 f(x_1, x_2, x_3, \varepsilon)\left[1 + \frac{1}{12} f(x_1, x_2, x_3, \varepsilon)^2\right] \tag{34}$$

The potential energy expressed by Eq. (34) is equal to the potential energy of the same arch when tilted by an angle $\omega = \tan^{-1}\varepsilon$ as shown by Eq. (13) and explained in the previous section. When the arch is tilted, all

Author's personal copy



conservative forces acting on the arch are now vertical and their work is accounted by the potential energy $V(x_1, x_2, x_3, \varepsilon)$ given by Eq. (34). According to the principle of stationary potential energy, the geometrically admissible hinge mechanism shown in Fig. 8 is in an equilibrium state if and only if the total potential energy of the arch is stationary ($\delta V = 0$). Since in this case, the potential energy $V(x_1, x_2, x_3, \varepsilon)$ is a function of three variables $x_1$, $x_2$ and $x_3$, and the potential energy is stationary when [25]

$$\frac{\partial V(x_1, x_2, x_3, \varepsilon)}{\partial x_1} = 0 \tag{35}$$

$$\frac{\partial V(x_1, x_2, x_3, \varepsilon)}{\partial x_2} = 0 \tag{36}$$

$$\frac{\partial V(x_1, x_2, x_3, \varepsilon)}{\partial x_3} = 0 \tag{37}$$

Substitution of Eq. (33) to any of the Eqs. (35)–(37) ($j \in \{1, 2, 3\}$) gives

$$\frac{\partial V(x_j, \varepsilon)}{\partial x_j} = 2 \sin\left(\frac{\beta}{2}\right) R^3 \frac{\partial f(x_j, \varepsilon)}{\partial x_j} \left[1 + \frac{1}{4} f(x_j, \varepsilon)^2\right] = 0, \quad j \in \{1, 2, 3\} \tag{38}$$

The quantity in brackets in Eq. (38) is always positive; therefore, Eq. (18) is satisfied only when $\frac{\partial f(x_j, \varepsilon)}{\partial x_j} = 0$. Accordingly, the tilting arch is in an limiting equilibrium state ($\delta V(x_1, x_2, x_3, \varepsilon) = 0$) if and only if all partial derivatives of the function $f(x_1, x_2, x_3, \varepsilon)$ given by Eq. (33) vanish

$$\frac{\partial f(x_1, x_2, x_3, \varepsilon)}{\partial x_1} = \frac{\partial (t/R)}{\partial x_1} = 0 \tag{39}$$

$$\frac{\partial f(x_1, x_2, x_3, \varepsilon)}{\partial x_2} = \frac{\partial (t/R)}{\partial x_2} = 0 \tag{40}$$

$$\frac{\partial f(x_1, x_2, x_3, \varepsilon)}{\partial x_3} = \frac{\partial (t/R)}{\partial x_3} = 0 \tag{41}$$

Numerical solution of the system of Eqs. (33) and (39)–(41) gives the unknown locations $x_1, x_2$ and $x_3$ of the three hinges (the location of the fourth hinge is known at the downstream springing A) together with the minimum thickness $t/R$ of a circular arch with a given angle of embrace $\beta$.

Figure 6 plots with a dashed line the minimum thickness values $t/R$ of a circular arch with a given angle of embrace $\beta$ when subjected to various levels of horizontal acceleration $\ddot{u}_g = \varepsilon g$. Note that the minimum thickness values obtained by assuming vertical ruptures are slightly larger than the minimum thickness values obtained when assuming radial rupture. Consequently, this work shows that the minimum thickness value of an arch that is needed to sustain a given horizontal acceleration depends on the stereotomy assumed for the creation of the hinged mechanism. Most importantly, this work shows that it is easier for a circular arch to form ruptures along the vertical direction, although these vertical ruptures are longer than the ruptures along the radial direction.

This multiplicity in the solution derives from the fact that a continuous monolithic arch has a finite thickness $t/R$; therefore, the geometry and weight of the articulated segments of the arch depend on the direction of the assumed ruptures—that is the stereotomy exercised. Figure 6 shows that for smaller embracing angles, $\beta$, the minimum thickness of the arch decreases; therefore, the difference between the solutions obtained either by assuming radial or vertical ruptures decreases. In the event of a masonry arch that consists of individual voussoirs with finite directions and discrete physical joints, the direction of the imminent ruptures is uniquely defined by the direction of the physical joints and the solution for the minimum thickness is unique.

Figure 9 plots the location of the imminent hinges of a circular arch with a given angle of embrace, $\beta$, when subjected to various levels of horizontal acceleration $\ddot{u}_g = \varepsilon g$ and when the direction of the rupture is assumed vertical.

To this end, Table 1 offers arithmetic values of the minimum thickness $t/R$ and the corresponding locations of the imminent hinges B, C and D of a circular arch to withstand a constant acceleration $\ddot{u}_g = \varepsilon\, g$.

The arithmetic values appearing in Table 1 are for an idealized geometry (no corner cracks) together with the assumption that there is no sliding between blocks. The possible collapse mechanism in a semicircular arch where both sliding and rocking happens has been examined in the work of Sinopoli et al. [27], and it was concluded that for values of the interface friction, $\mu > 0.4$ sliding along the interface is excluded and only the

Author's personal copy



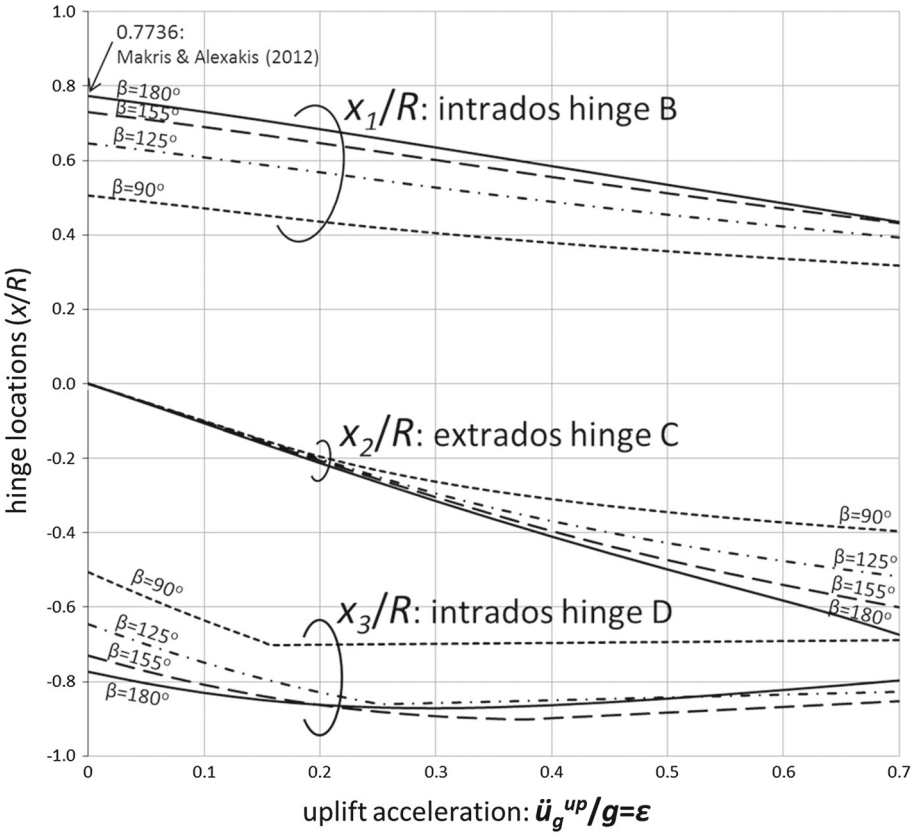



**Fig. 9** Location of the imminent hinges, $x_1$, $x_2$, and $x_3$, at points B, C and D of a circular arch with embrace angle $\beta$ and minimum thickness $t/R$ as shown in Fig. 6 (*dashed lines*) that ruptures along the vertical direction when subjected to a constant horizontal acceleration $\ddot{u}_g = \varepsilon g$

rocking mechanism prevails. Given that for limestone and marble arches, the coefficient of interface friction is above 0.7 ($\mu > 0.7$, [28]), and the possibility of sliding along some interface joint becomes remote. On the other hand, at the initiation of uplifting of a masonry arch, the corners of the voussoirs at the hinge locations are subjected to high compressive stresses that induce plastic deformations and eventually local damage. Given this behavior, the minimum thickness values appearing in Table 1 shall be understood as theoretical lower bounds and not as design values.

## 3 The distinct element method

During the last two decades, an increasing number of researchers are using the distinct element method (DEM) for modeling and analyzing masonry structures [28–33, among others]. The software UDEC v4.0 [26] simulates the response of discontinuous media (such as a jointed rock mass) subjected to either static or dynamic loading. In the distinct element method, a structural system is represented as an assembly of discrete blocks. The method works in terms of forces and displacements, and each block is treated as a separate entity, allowed to undergo unlimited translation and rotation. At every time step, the calculations satisfy force and moment equilibrium. The method adopts an elastic behavior which leads to the need to define the normal-to-the contact surface, $K_n$ (normal stiffness), and the tangential-to-the contact surface, $K_s$ (shear stiffness), equivalent linear elastic constants. The discontinuities are treated as boundary conditions between blocks, whereas large displacements along discontinuities and rotations of blocks are allowed.

In this numerical analysis, the spring constants assume the value $K_n = K_s = 10^9$ Pa/m $= 1$ MPa/mm, while the angle of internal friction has been assumed large enough to not allow any sliding. Upon sliding has been prevented, our analysis concludes that the results are insensitive to the exact values of $K_n$ and $K_s$.

Author's personal copy



**Table 1** Values of the minimum thickness $t/R$ and locations of the imminent hinges B, C and D of a circular arch with embrace angle $\beta$ to withstand a constant horizontal acceleration $\ddot{u}_g = \varepsilon g$

| $\varepsilon$ | Radial ruptures | | | | Vertical ruptures | | | |
|---|---|---|---|---|---|---|---|---|
| | $\beta = 180°$ | | | | $\beta = 180°$ | | | |
| | $t/R$ | $\varphi_1(°)$ | $\varphi_2(°)$ | $\varphi_3(°)$ | $t/R$ | $x_1/R$ | $x_2/R$ | $x_3/R$ |
| 0.0 | 0.10748 | 35.516 | 90.000 | 144.484 | 0.10946 | 0.7736 | 0.0000 | −0.7736 |
| 0.1 | 0.13590 | 38.894 | 95.710 | 152.528 | 0.13936 | 0.7310 | −0.1064 | −0.8303 |
| 0.2 | 0.16897 | 42.412 | 101.310 | 160.208 | 0.17446 | 0.6843 | −0.2124 | −0.8625 |
| 0.3 | 0.20636 | 46.025 | 106.699 | 167.373 | 0.21429 | 0.6352 | −0.3146 | −0.8717 |
| 0.4 | 0.24752 | 49.693 | 111.801 | 173.910 | 0.25799 | 0.5850 | −0.4101 | −0.8636 |
| 0.5 | 0.29175 | 53.389 | 116.565 | 179.741 | 0.30469 | 0.5349 | −0.4983 | −0.8457 |
| 0.6 | **0.33788** | **57.063** | **120.852** | **180 (2SM)** | 0.35394 | 0.4852 | −0.5822 | −0.8227 |
| 0.7 | **0.38495** | **60.705** | **124.617** | **180 (2SM)** | 0.40608 | 0.4349 | −0.6739 | −0.7970 |
| | $\beta = 155°$ | | | | $\beta = 155°$ | | | |
| | $t/R$ | $\varphi_1(°)$ | $\varphi_2(°)$ | $\varphi_3(°)$ | $t/R$ | $x_1/R$ | $x_2/R$ | $x_3/R$ |
| 0.0 | 0.06083 | 41.257 | 90.000 | 138.743 | 0.06132 | 0.7303 | 0.0000 | −0.7303 |
| 0.1 | 0.07974 | 44.244 | 95.711 | 147.177 | 0.08066 | 0.6902 | −0.1035 | −0.8085 |
| 0.2 | 0.10217 | 47.337 | 101.310 | 155.283 | 0.10373 | 0.6469 | −0.2060 | −0.8629 |
| 0.3 | 0.12789 | 50.480 | 106.699 | 162.918 | 0.13025 | 0.6015 | −0.3043 | −0.8931 |
| 0.4 | **0.15638** | **53.611** | **111.761** | **167.5 (2SM)** | **0.15953** | **0.5558** | **−0.3952** | **−0.8984 (2SM)** |
| 0.5 | **0.18607** | **56.567** | **116.083** | **167.5 (2SM)** | **0.19013** | **0.5121** | **−0.4731** | **−0.8835 (2SM)** |
| 0.6 | **0.21627** | **59.343** | **119.737** | **167.5 (2SM)** | **0.22138** | **0.4709** | **−0.5400** | **−0.8682 (2SM)** |
| 0.7 | **0.24671** | **61.983** | **122.900** | **167.5 (2SM)** | **0.25314** | **0.4317** | **−0.6003** | **−0.8527 (2SM)** |
| | $\beta = 125°$ | | | | $\beta = 125°$ | | | |
| | $t/R$ | $\varphi_1(°)$ | $\varphi_2(°)$ | $\varphi_3(°)$ | $t/R$ | $x_1/R$ | $x_2/R$ | $x_3/R$ |
| 0.0 | 0.02673 | 49.133 | 90.000 | 130.867 | 0.02679 | 0.6459 | 0.0000 | −0.6459 |
| 0.1 | 0.03737 | 51.728 | 95.711 | 139.693 | 0.03751 | 0.6085 | −0.1014 | −0.7489 |
| 0.2 | 0.05051 | 54.411 | 101.310 | 148.209 | 0.05079 | 0.5684 | −0.2010 | −0.8290 |
| 0.3 | **0.06592** | **57.093** | **106.578** | **152.5 (2SM)** | **0.06637** | **0.5273** | **−0.2943** | **−0.8576 (2SM)** |
| 0.4 | **0.08225** | **59.522** | **110.792** | **152.5 (2SM)** | **0.08294** | **0.4892** | **−0.3685** | **−0.8502 (2SM)** |
| 0.5 | **0.09899** | **61.707** | **114.136** | **152.5 (2SM)** | **0.09993** | **0.4546** | **−0.4274** | **−0.8427 (2SM)** |
| 0.6 | **0.11588** | **63.702** | **116.882** | **152.5 (2SM)** | **0.11713** | **0.4227** | **−0.4759** | **−0.8351 (2SM)** |
| 0.7 | **0.13277** | **65.548** | **119.215** | **152.5 (2SM)** | **0.13439** | **0.3931** | **−0.5176** | **−0.8274 (2SM)** |
| | $\beta = 90°$ | | | | $\beta = 90°$ | | | |
| | $t/R$ | $\varphi_1(°)$ | $\varphi_2(°)$ | $\varphi_3(°)$ | $t/R$ | $x_1/R$ | $x_2/R$ | $x_3/R$ |
| 0.0 | 0.00750 | 59.485 | 90.000 | 120.515 | 0.00750 | 0.5059 | 0.0000 | −0.5059 |
| 0.1 | 0.01193 | 61.692 | 95.711 | 129.729 | 0.01194 | 0.4715 | −0.1001 | −0.6354 |
| 0.2 | **0.01781** | **63.928** | **101.145** | **135 (2SM)** | **0.01783** | **0.4358** | **−0.1950** | **−0.7008 (2SM)** |
| 0.3 | **0.02435** | **65.827** | **105.050** | **135 (2SM)** | **0.02439** | **0.4049** | **−0.2627** | **−0.6985 (2SM)** |
| 0.4 | **0.03116** | **67.406** | **107.758** | **135 (2SM)** | **0.03122** | **0.3788** | **−0.3096** | **−0.6961 (2SM)** |
| 0.5 | **0.03807** | **68.763** | **109.771** | **135 (2SM)** | **0.03817** | **0.3561** | **−0.3444** | **−0.6936 (2SM)** |
| 0.6 | **0.04500** | **69.965** | **111.372** | **135 (2SM)** | **0.04515** | **0.3359** | **−0.3723** | **−0.6911 (2SM)** |
| 0.7 | **0.05192** | **71.056** | **112.717** | **135 (2SM)** | **0.05212** | **0.3175** | **−0.3958** | **−0.6887 (2SM)** |

The bold values correspond to the development of a two-springing, four-hinge mechanism (2SM). The minimum thickness values derived after assuming vertical ruptures are larger than the corresponding values after assuming radial ruptures; therefore vertical ruptures are most critical

The results from the software UDEC v4.0 [26] presented in Fig. 6 (dotted lines) are for Vitruvius voussoirs with size = 5° as shown in Fig. 10. Accordingly, the semicircular arch has 36 voussoirs, whereas the arch with embracing angle $\beta = 90°$ has 18 voussoirs. The gravity load and horizontal inertia load corresponding to each voussoir have been applied as static loads at the center of gravity of each voussoir. Figure 10 shows snapshots from the initiation of collapse when the arches assume their critical thickness, $t/R$, when the seismic coefficient, $\varepsilon = 0.3(\ddot{u}_g = 0.3\text{g})$. The two top arches with $\beta = 180°$ and $\beta = 155°$ develop a one-springing, 4-hinge mechanism, whereas the two bottom arches with $\beta = 125°$ and $\beta = 90°$ develop a two-springing, 4-hinge mechanism. Given that Vitruvius voussoirs have radial joints, the numerical solution of UDEC is in excellent agreement with the theoretical solution from the variational formulation when radial ruptures are assumed.

The reader may recognize that when a circular arch is constructed with smaller stone blocks where the size of the block is smaller than the thickness of the arch, the physical rupture of the arch will occur along the most critical direction which according to this analysis is the vertical direction.

Author's personal copy



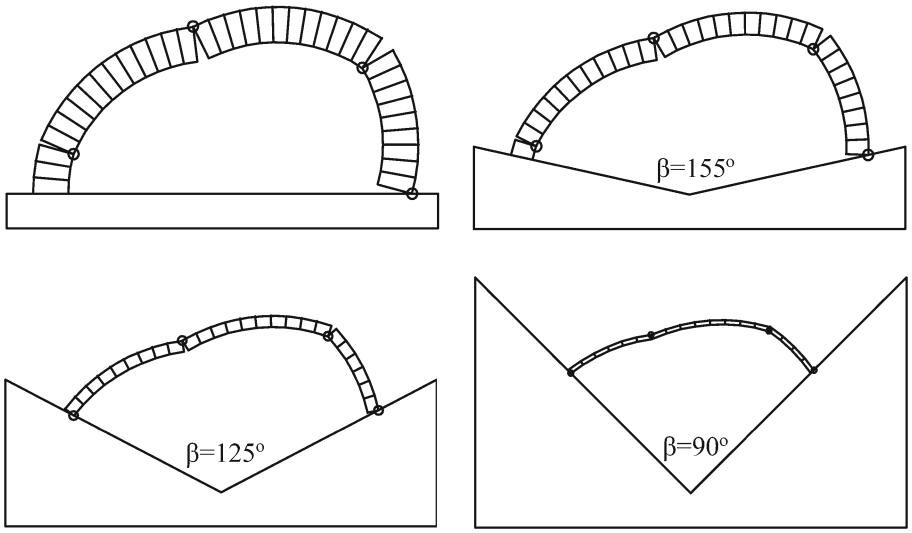



**Fig. 10** Initiation of collapse of circular arches with 5° voussoirs and various embracing angles $\beta = 180°, 155°, 125°, 90°$ subjected to a constant horizontal acceleration $\ddot{u}_g = 0.3g$ ($\varepsilon = 0.3$) in association with their gravity load as predicted with the software UDEC v4.0. The gravity load ($1g$) and the horizontal inertia load ($0.3g$) are applied as static loads at the center of gravity of each voussoir

## 4 Conclusions

This paper revisits the limit equilibrium analysis of a continuous monolithic circular arch with zero tensile strength when subjected to a given level of a horizontal ground acceleration $\varepsilon\, g$. The main finding of this paper is that the minimum thickness of the arch and the locations of the imminent hinges depend on the directions of the ruptures that the arch with finite thickness develops when it converts into a mechanism.

This result is obtained with a variational formulation and the application of the principle of stationary potential energy. The paper concludes that the multiplicity in the solutions for the minimum thickness, $t/R$, derives from the infinite many possible directions that the arch may rupture upon hinging has initiated (multiplicity in stereotomy). Each possible direction of rupturing defines distinct shapes/weights of the macroscopic articulated segments of the arch and the minimum thickness, $t/R$, of the arch together with the locations of the imminent hinges as derived from the application of the principle of stationary potential energy, depends on the exact shape/weight of the articulated segment considered.

Interestingly, this work shows that it is easier for a circular arch to form ruptures along the vertical direction, although these vertical ruptures are longer than the alternative ruptures along the radial direction.

Finally, this paper shows that numerical results from distinct element method (DEM) are in very good agreement with the theoretical solution presented in this work derived with a variational formulation.

**Acknowledgments** This work was funded by the research project "SeismoRockBridge" No 2295 which is implemented under the "ARISTEIA" Action of the "OPERATIONAL PROGRAMME EDUCATION AND LIFELONG LEARNING" and is co-funded by the European Social Fund (ESF) and Greek National Resources.

## References

1. Couplet, P.: De la poussée des voûtes. Histoire de l'Académie Royale des Sciences, Paris (1729, 1730)
2. Milankovitch, M.: Beitrag zur Theorie der Druckkurven. Dissertation zur Erlangung der Doktorwürde, K.K. technische Hochschule, Vienna (1904)
3. Milankovitch, M.: Theorie der Druckkurven. Zeitschrift für Mathematik Und Physik **55**, 1–27 (1907)
4. Heyman, J.: The safety of masonry arches. Int. J. Mech. Sci. **11**, 363–385 (1969). doi:10.1016/0020-7403(69)90070-8
5. Foce, F.: On the safety of the masonry arch. Different formulations from the history of structural mechanics. In: Huerta, S. (ed.) Essays in the History of Theory of Structures, pp. 117–142. Instituto Juan de Herrera, Madrid (2005)
6. Foce, F.: Milankovitch's Theorie der Druckkurven: good mechanics for masonry architecture. Nexus Netw. J. **9**, 185–210 (2007). doi:10.1007/s00004-007-0039-9
7. Albuerne, A., Huerta, S.: Coulomb's theory of arches in Spain ca. 1800: the manuscript of Joaquín Monasterio. In: Chen, B., Wei, J. (eds.) In: Proc. 6th Int. Conf. on Arch Bridges (ARCH'10). Fuzhou, China, pp. 354–362 (2010)

Author's personal copy




8. Oppenheim, I.J.: The masonry arch as a four-link mechanism under base motion. Earthq. Eng. Struct. Dyn. **21**, 1005–1017 (1992). doi:10.1002/eqe.4290211105
9. Konstantinidis, D., Makris, N.: Experimental and analytical studies on the response of freestanding laboratory equipment to earthquake shaking. Earthq. Eng. Struct. Dyn. **38**, 827–848 (2009). doi:10.1002/eqe.871
10. Makris, N., Vassiliou, M.F.: Sizing the slenderness of free-standing rocking columns to withstand earthquake shaking. Arch. Appl. Mech. **82**, 1497–1511 (2012). doi:10.1007/s00419-012-0681-x
11. Makris, N., Vassiliou, M.F.: Planar rocking response and stability analysis of an array of free-standing columns capped with a freely supported rigid beam. Earthq. Eng. Struct. Dyn. **42**, 431–449 (2013). doi:10.1002/eqe.2222
12. Clemente, P.: Introduction to dynamics of stone arches. Earthq. Eng. Struct. Dyn. **27**, 513–522 (1998). doi:10.1002/(SICI)1096-9845(199805)27:5$<$513::AID-EQE740$>$3.0.CO;2-O
13. De Lorenzis, L., DeJong, M., Ochsendorf, J.: Failure of masonry arches under impulse base motion. Earthq. Eng. Struct. Dyn. **36**, 2119–2136 (2007). doi:10.1002/eqe.719
14. De Jong, M., De Lorenzis, L., Adams, S., Ochsendorf, J.: Rocking stability of masonry arches in seismic regions. Earthq. Spectra **24**, 847–865 (2008). doi:10.1193/1.2985763
15. De Luca, A., Giordano, A., Mele, E.: A simplified procedure for assessing the seismic capacity of masonry arches. Eng. Struct. **26**, 1915–1929 (2004). doi:10.1016/j.engstruct.2004.07.003
16. Ochsendorf, J.: Collapse of Masonry Structures. PhD Dissertation, Department of Engineering, University of Cambridge, Cambridge (2002)
17. Makris, N., Alexakis, H.: From Hooke's "Hanging Chain" and Milankovitch's "Druckkurven" to a Variational Formulation: The Adventure of the Thrust-Line of Masonry Arches. Report series in EEAM 2012-02. University of Patras, Greece (2012)
18. Makris, N., Alexakis, H.: The effect of stereotomy on the shape of the thrust-line and the minimum thickness of semicircular masonry arches. Arch. Appl. Mech. **83**, 1511–1533 (2013). doi:10.1007/s00419-013-0763-4
19. Alexakis, H., Makris, N.: Minimum thickness of elliptical masonry arches. Acta Mech. **224**, 2977–2991 (2013). doi:10.1007/s00707-013-0906-2
20. Lamé, M.G., Clapeyron, E.: Mémoire sur la stabilité des voûtes. Annales Des Mines **8**, 789–836 (1823)
21. Timoshenko, S.P.: History of Strength of Materials. McGraw-Hill, New York (1953)
22. Heyman, J.: La Coupe des Pierres. In: Kurrer, K.E., Lorenz, W., Wetzk, V. (eds.) Proc. 3rd Int. Cong. on Construction History. Neunplus1, Berlin, 2, pp. 807–812 (2009)
23. Gaß, S.: IL 25: Experiments. University of Lightweight Structures. Institute for Lightweight Structures, Germany (1990)
24. De Jong, M.: Seismic Assessment Strategies for Masonry Structures. PhD dissertation. Department of Architecture. Massachusetts Institute of Technology, USA (2009)
25. Shames, I.H., Dym, C.L.: Energy and Finite Elements Methods in Structural Mechanics. Hemisphere Publishing Corporation, New York (1985)
26. UDEC: Universal Distinct Element Code, v.4.0. Itasca Consulting Group, Inc., Minneapolis (2004)
27. Sinopoli, A., Corradi, M., Foce, F.: Modern formulation for preelastic theories on masonry arches. J. Eng. Mech. **123**, 204–213 (1997). doi:10.1061/(ASCE)0733-9399(1997)123:3(204)
28. Alexakis, H., Makris, N.: Structural stability and bearing capacity analysis of the tunnel-entrance to the stadium of ancient Nemea. Int. J. Arch. Herit. **7**, 673–692 (2013). doi:10.1080/15583058.2012.662262
29. Cundall, P.A.: A computer model for simulating progressive large-scale movements in blocky rock system. In: Proceedings of the Symposium of the International Society for Rock Mechanics, vol. I. Nancy, France, n.II-8 (1971)
30. Pagnoni, T., Vanzi, I.: Experimental and numerical study of the seismic response of block structures. In: Middleton, J., Pande, G.N. (eds.) Computer Methods in Structural Masonry, pp. 213–222. Books & Journals International, Swansea (1995)
31. Lemos, J.V.: Assessment of the ultimate load of a masonry arch using discrete elements. In: Middleton, J., Pande, G.N. (eds.) Computer Methods in Structural Masonry, pp. 294–302. Books & Journals International, Swansea (1995)
32. Lemos, J.V.: Discrete element modelling of masonry structures. Int. J. Arch. Herit. **1**, 190–213 (2007). doi:10.1080/15583050601176868
33. Papantonopoulos, C., Psycharis, I.N., Papastamatiou, D.Y., Lemos, J.V., Mouzakis, H.P.: Numerical prediction of the earthquake response of classical columns using the distinct element method. Earthq. Eng. Struct. Dyn. **31**, 1699–1717 (2002). doi:10.1002/eqe.185